Pseudogap in underdoped cuprates and spin-density-wave fluctuations

Tigran A. Sedrakyan[1,2] and Andrey V. Chubukov[1]

[1]*Department of Physics, University of Wisconsin–Madison, Madison, Wisconsin 53706, USA*
[2]*Department of Physics, University of Maryland, College Park, Maryland 20742, USA*

We analyze fermionic spectral function in the spin-density-wave (SDW) phase of quasi-two-dimensional (quasi-2D) cuprates at small but finite T. We use a nonperturbative approach and sum up infinite series of thermal self-energy terms, keeping at each order nearly divergent $(T/J)|\log \epsilon|$ terms, where ϵ is a deviation from a pure 2D, and neglecting regular T/J corrections. We show that, as SDW order decreases, the spectral function in the antinodal region acquires peak/hump structure: the coherent peak position scales with SDW order parameter while the incoherent hump remains roughly at the same scale as at $T=0$ when SDW order is the strongest. We identify the hump with the pseudogap observed in angle-resolved photoemission spectroscopy and argue that the presence of coherent excitations at low energies gives rise to magneto-oscillations in an applied field. We show that the same peak/hump structure appears in the density of states and in optical conductivity.

I. INTRODUCTION

Understanding of the phase diagram of cuprate superconductors continue to be one of central topics in theoretical condensed-matter physics.[1] Parent compounds of cuprates are quasi-two-dimensional (quasi-2D) antiferromagnetic insulators, heavily overdoped cuprates are Fermi liquids. In between, systems are d-wave superconductors at low $T<T_c$ and display the pseudogap behavior at larger $T_c<T<T^*$. How an insulator transforms into a Fermi liquid and what is the origin of the pseudogap are still the subjects of intensive debates among researchers.

The pseudogap region exists both in underdoped and overdoped cuprates, but the physics evolves substantially between these two limits. For overdoped cuprates, there is rather strong evidence[2] that the pseudogap region is best described as a disordered superconductor, when the gap is already developed but the phase coherence is not yet set.[3–6] In this doping range, fermions are reasonably well described as strongly interacting quasiparticles with a large, Luttinger-type underlying Fermi surface (FS).[7] The d-wave pairing in this doping range most naturally originates from the exchange of overdamped collective bosonic excitations of which spin-fluctuation-mediated pairing is the key candidate.[7–11] In underdoped cuprates, situation is more complex. On one hand, angle-resolved photoemission spectroscopy (ARPES) data taken at low energies (below 50 meV) and low T were interpreted as the indication that the underlying FS still has Luttinger form, and the gap extracted from the position of the still visible narrow peak in the spectral function has a simple d wave, $\cos 2\phi$ form over the whole FS, including antinodal region around $(0,\pi)$ and symmetry-related points.[12,13] On the other hand, ARPES data taken in the antinodal region show that the spectral function in the pseudogap regime develops a broad maximum at around 100–200 meV.[13–15] The jury is still out[16] whether the observed high-energy hump and low-energy peak are separate features or the peak and the hump describe the same gap, $\Delta(k)$, which strongly deviates from $\cos 2\phi$ form with under-

doping. The experimental results in Refs. 13–15 and 17–20 were interpreted both ways. We side with the idea that the pairing gap remains $\cos 2\phi$ even in underdoped materials, and the hump is a separate feature, associated with Mott physics. We further take the point of view that the origin of the hump is the development of precursors to a Heisenberg-like antiferromagnetically ordered state at half-filling.[21–28] These precursors are generally termed as spin-density-wave (SDW) precursors though one should keep in mind that the half-filled state is the strong coupling version of SDW and is best described by the Heisenberg model with short-range exchange interaction. The SDW precursor scenario has been wildly discussed in mid-90s,[21,23,29,30] and is nearly universally accepted scenario for electron-doped cuprates[24,25,31] For hole-doped cuprates, it was, however, put aside for a number of years if favor of non-Fermi-liquid-type scenarios.[32] The SDW scenario, however, regained support in the last few years, after magneto-oscillation experiments in a field of 30–60 T detected long-lived Fermi-liquid quasiparticles near small electron and hole FSs.[33] Such FS geometry is expected for an SDW ordered state,[21] and early theory prediction was that a field drives the system toward an SDW instability.[34] Long-range antiferromagnetic order in applied field has been explicitly detected in recent neutron-scattering experiments on underdoped YBCO (Ref. 35). (Another widely discussed scenario of quantum oscillations, which we will not consider here, is a d-wave density-wave order.[36])

In this paper, we analyze the consistency between the description of quantum oscillations *and* the pseudogap in underdoped cuprates within SDW scenario. The problem is the following: to explain quantum oscillations one has to assume the existence of small electron pockets.[37,38] Such pockets do exist in the SDW scenario near $(0,\pi)$ and symmetry-related points, but they are present only if SDW order $\langle S_z(Q) \rangle = \langle S_z \rangle$ is smaller than a threshold $[Q=(\pi,\pi)]$. For larger $\langle S_z \rangle$, only hole pockets around $(\pi/2,\pi/2)$ are present, while excitations near $(0,\pi)$ have a gap of order $4t' \sim 0.2$ eV (see Fig. 2). Antinodal pseudogap detected in ARPES experiments in zero field is of the same magnitude.[13] A field of

40–60 T is too small to affect energies of 0.2 eV, hence the same 200 meV pseudogap should be present in the ordered SDW state.[39] If this pseudogap is viewed as a precursor to SDW, one could expect that it simply sharpens up in the ordered SDW phase and transforms into the true antinodal gap. But then there will be no electron pockets in the SDW phase, in disagreement with magneto-oscillation experiments. The pseudogap and quantum oscillations can be reconciled within SDW scenario only if the evolution of the spectral function between paramagnetic and SDW states is more complex than just the sharpening of the pseudogap, and antinodal spectral function in the SDW phase contains both high-energy pseudogap and electron pockets. This coexistence also explains ARPES data in the superconducting state[12,13] because pairing of coherent fermions near electron pockets gives rise to a sharp peak in the spectral function at the gap energy.

To address this issue, we consider how fermionic Green's function $G(k,\omega)$ evolves within SDW phase, as SDW order gets smaller. We depart from Heisenberg antiferromagnet with exchange interaction $J=4t^2/U$ and consider analytically how $G(k,\omega)$ is affected by thermal fluctuations which in quasi-2D systems destroy long-range order already at $T \ll J$. We neglect regular T/J corrections but sum up infinite series of self-energy terms which contain powers of $\beta = (T/\pi J)|\log \epsilon|$, where ϵ is a parameter which measures deviations from pure two dimensionality and which we will just use as a lower cutoff of logarithmically divergent 2D integrals. In practice, is the ratio of the hoppings along z-axis and in xy plane.[40] SDW order disappears when $\beta = \beta_{cr} = O(1)$. This yields a set of integral equations for the Green's function and $\langle S_z \rangle$ which we obtain and solve.

In the terminology of Ref. 41, our computations are valid in the renormalized-classical regime of quasi-2D systems. The idea that, in this regime, at low enough T, one cannot restrict with Eliashberg or fluctuation exchange (FLEX) approximations and has to include self-energy and vertex corrections on equal footings has been put forward in Refs. 21 and 23. The computational procedure that we are using is similar to eikonal approximation in the scattering theory. Such procedure has been used in the study one-dimensional (1D) charge-density wave systems by Sadovskiic[42] and others[43] and has been applied to cuprates in Ref. 22 to analyze SDW precursors in the paramagnetic phase (for latest developments, see Ref. 26). Our computation has one advantage over earlier works: in the SDW-ordered state we do not need to assume that T is larger than some threshold T_0 to restrict with only thermal fluctuations (i.e., with the contributions from zero Matsubara frequency). All we need is a small ϵ such that $T/J|\log \epsilon| = O(1)$ even when T/J is small. In a paramagnetic phase, eikonal approximation is only valid when $T > T_0$, and T_0 increases as one moves away from the SDW phase. We assume that near SDW boundary T_0 is small and apply our theory also to a paramagnetic phase. Our results for a paramagnet are in full agreement with Ref. 22.

Note that in our theory (and in Ref. 22), the paramagnetic state is a Fermi liquid at the lowest energies at $T=0$. We do not discuss here a possibility that a new, non-Fermi-liquid state emerges near the region where SDW order is lost.[44] We also do not discuss possibilities of more complex spin order

and of open electron Fermi surfaces. Our results are expected to survive if SDW order is incommensurate, with **Q** still near (π, π), but whether our results survive if the system develops a stripe order remains to be seen.

We found that the spectral function $A(k, \omega) = (1/\pi)|\text{Im } G(k, \omega)|$ near $(0, \pi)$ in the SDW state has a peak and a hump. Both originate from a single peak at the value of the $T=0$ SDW gap at $(0, \pi)$. The hump moves little as SDW order decreases and just gets broader, while the peak follows $\langle S_z \rangle$, shifts to lower energies as SDW order decreases, and vanishes $\beta = \beta_{cr}$, when the system enter the paramagnetic phase. At $\beta \gtrsim \beta_{cr}$, only the hump (the pseudogap) remains, and the spectral function at antinodal $k=k_F$ has camel-like structure with a minimum at $\omega=0$. As β increases further, $A(k_F, \omega=0)$ increases and eventually the spectral function at $k=k_F$ develops a single peak at $\omega=0$, as it should be for a system with a large, Luttinger FS.

Rewinding this backward, from a paramagnet to an SDW state, we see that the system first develops a pseudogap as a precursor to SDW. When SDW order sets in, the pseudogap sharpens up, but, in addition, there also appears a true quasiparticle peak at low energies. The residue of the peak increases as $\langle S_z \rangle$ increases. When $\langle S_z \rangle$ is below the threshold, electron pockets are present, and the spectral function near $(0, \pi)$ has a low-energy coherent peak and a hump at about the same energy as the pseudogap in a paramagnetic phase. When SDW order gets larger, electron pockets eventually disappear, peak and hump come closer to each other and merge when $\langle S_z \rangle$ reaches its maximum.

This peak/hump structure also shows up in the density of states and in the optical conductivity $\sigma(\omega)$. In the Mott-Heisenberg limit ($2U\langle S_z \rangle$ is larger than free-fermion bandwidth) the conductivity at $T=0$ is zero up to a charge-transfer gap $U \sim 1.7$ eV. Once SDW order gets smaller, the peak at U splits into a hump which slowly shifts to a higher frequency, and a peak whose energy scales as $2U\langle S_z \rangle$. In addition, there appears a metallic Drude component at the smallest frequencies. This behavior is quite consistent with the measured $\sigma(\omega)$ in electron-doped cuprates, where SDW phase extends over a substantial doping range.[44–47]

We also found that, at a finite T, the system in the pseudogap phase retains the memory about pockets. There are no real pockets in the sense that there is no two-peak structure of the spectral function at zero frequency along zone diagonal, but we found that, when $\beta \gtrsim \beta_{cr}$, the spectral weight at $\omega=0$ extends almost all the way between the original FS at k_F and the "shadow" FS at $k=Q-k_F$ (see Fig. 8). As β becomes larger, the k range where the spectral weight is finite shrinks and at large β the spectral function recovers Drude-type structure typical for a metal with a large, Luttinger FS.

This analysis can be extended into a superconducting state. A system does not need to possess coherent quasiparticles to develop a pairing instability,[48,49] but fermionic coherence emerges below the actual T_c much in the same way as it emerges in the SDW ordered state. The spectral function in the antinodal region then displays a coherent superconducting peak and a hump centered at, roughly, the energy of the antinodal SDW gap at $T=0$. This picture is consistent with the data from Refs. 13 and 18.
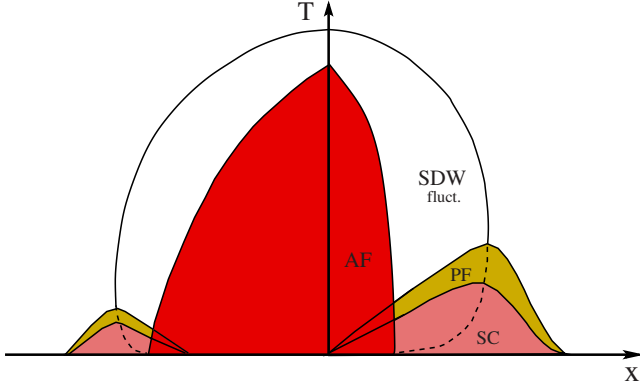
FIG. 1. (Color online) Schematic phase diagram of hole- and electron-doped cuprates. The regions of antiferromagnetism (AF), superconductivity (SC), and pairing fluctuations (PF) are shaded. In the PF region, there are vortex excitations and large Nernst signal (Ref. 50). Precursors to SDW appear at a nonzero T due to strong thermal fluctuations. In the region where SDW precursors are already developed, the onset temperature for the pairing increases with increasing x (Ref. 51), in the region with no SDW precursors, it decreases with increasing x (Ref. 7), the maximum T_c is in the area between the two regimes. A similar phase diagram has been proposed in Ref. 52.

The overall conclusion of our analysis is the phase diagram of the cuprates presented in Fig. 1. A similar phase diagram has been proposed in Ref. 52. At $T \neq 0$, there is a region where the system displays SDW precursors. In this region, magnetic excitations are moderately damped, propagating magnons, and magnetically mediated d-wave pairing interaction decrease as doping decreases due to a reduction in the electron-magnon vertex.[51,53,54] In this region, the antinodal pseudogap, caused by SDW precursors, and a d-wave pairing gap coexist. Outside this region, SDW precursors do not emerge, and arcs and other pseudogap features are caused by thermal fluctuations of a pairing gap.[5,17,55]

We discuss the computational procedure in the next section, present the results in Sec. III and conclusions in Sec. IV.

II. COMPUTATIONAL PROCEDURE

Our point of departure is the mean-field, SDW theory[21,56–58] of the antiferromagnetically ordered state in the large U quasi-2D Hubbard model at $T=0$. We assume $t-t'$ dispersion in the XY plane [$\epsilon_k = -2t(\cos k_x + \cos k_y) - 4t' \cos k_x \cos k_y$] and weak dispersion along the Z axis, which we will not keep explicitly in the formulas. Mean-field description neglects quantum fluctuations and is rigorously justified when the model is extended to $2S \gg 1$ fermionic flavors,[59] but qualitatively it remains valid even for $S = 1/2$ ($\langle S_z \rangle$ becomes 0.32 instead of 0.5).

Long-range antiferromagnetic order splits the fermionic dispersion into valence and conduction bands, separated by U, and gives rise to a two-pole structure of the bare fermionic Green's function

$$G_0(\omega, \mathbf{k}) = u_k^2 G_0^c + v_k^2 G_0^v, \qquad (1)$$

where $u_k, v_k = \sqrt{(1 \mp 4t\gamma_k/E_k)/2}$, $\gamma_k = (\cos k_x + \cos k_y)/2$, and
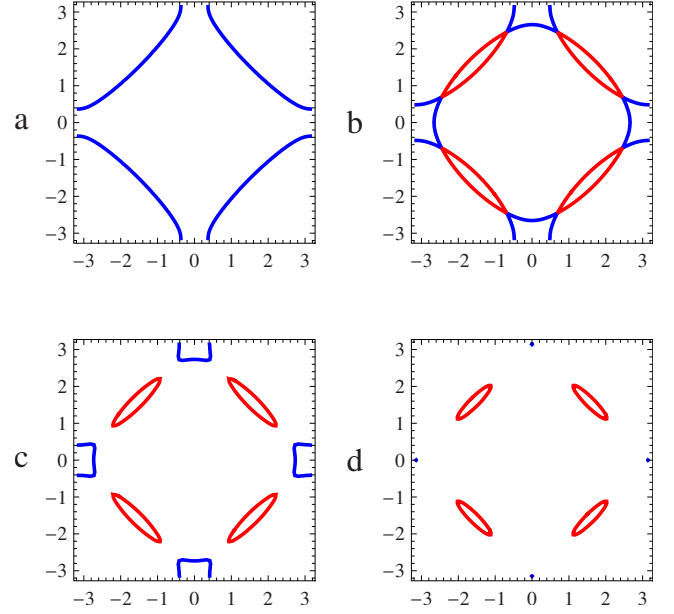

FIG. 2. (Color online) Evolution of the FS with increasing SDW order. (a)—paramagnetic phase; (b)—SDW order is about to develop ($\langle S_z \rangle = 0^+$). The shadow FS emerges, but the residue of fermionic excitations at the shadow FS is 0^+; (c)—small $\langle S_z \rangle$, both hole and electron pockets are present; (d)—a larger $\langle S_z \rangle$, only hole pockets around $(\pi/2, \pi/2)$ remain.

$$G_0^c = \frac{1}{\omega - E_k^c}, \quad G_0^v = \frac{1}{\omega - E_k^v}. \qquad (2)$$

The dispersions of conduction and valence electrons are given by $E_k^{c,v} = \pm E_k - 4t' \cos k_x \cos k_y - \mu$, where $E_k = [\Delta_0^2 + 16t^2\gamma_k^2]^{1/2}$, $\Delta_0 = U\langle S_z \rangle$, and $\mu \approx -\Delta_0$ is the chemical potential.

The shape of the FS depends on the value of Δ_0. We show the evolution of the FS with increasing Δ_0 in Fig. 2. For small Δ_0 both hole and electron pockets are present, for larger Δ_0 only hole pockets remain. At large U/t, which we assume to hold, valence, and conduction bands are well separated near half-filling at $T=0$, $u_k^2 \approx v_k^2 \approx 1/2$, and the FS only contains hole pockets.

The value of $\langle S_z \rangle$ is determined by the self-consistency condition

$$\langle S_z \rangle = \int \frac{d^2k}{(2\pi)^2} u_k v_k \int \frac{d\omega}{\pi} n_F(\omega) \text{Im}[G_0^c - G_0^v], \qquad (3)$$

where both G_0^c and G_0^v are retarded functions and $n_F(\omega)$ is the Fermi function. At large U, and near half-filling, $\langle S_z \rangle \approx 1/2$, and $\Delta_0 \approx U/2$. For larger dopings and smaller U, $\langle S_z \rangle$ is smaller already at $T=0$.

Fermion-fermion interactions in the ordered SDW state can be cast into interactions between fermions and magnons. These interactions are described by the effective Hamiltonian[21]

$$H_{el\text{-}mag} = \sum_{\alpha,\beta} \sum_{k,q} [a_{\alpha k}^+ a_{\beta k+q} e_q^+ V_{aa}(k,q) + b_{\alpha k}^+ b_{\beta k+q} e_q^+ V_{bb}(k,q)$$
$$+ a_{\alpha k}^+ b_{\beta k+q} e_q^+ V_{ab}(k,q) + b_{\alpha k}^+ a_{\beta k+q} e_q^+ V_{ba}(k,q)$$
$$+ \text{H.c.}]\delta_{\alpha,-\beta}, \tag{4}$$

where operators a and b represent conduction- and valence-band fermions, respectively. The vertex functions are given by

$$V_{aa,bb}(k,q) = \frac{U}{\sqrt{2}}[\pm(u_k u_{k+q} - v_k v_{k+q})\eta_q + (u_k v_{k+q}$$
$$- v_k u_{k+q})\bar{\eta}_q],$$

$$V_{ab,ba}(k,q) = \frac{U}{\sqrt{2}}[(u_k v_{k+q} + v_k u_{k+q})\eta_q \mp (u_k u_{k+q} + v_k v_{k+q})\bar{\eta}_q] \tag{5}$$

with

$$\eta_q = \frac{1}{\sqrt{2}}\left(\frac{1 - \gamma_q}{1 + \gamma_q}\right)^{1/4}, \quad \bar{\eta}_q = \frac{1}{\sqrt{2}}\left(\frac{1 + \gamma_q}{1 - \gamma_q}\right)^{1/4}. \tag{6}$$

At the mean-field level, the spectral function $A(k,\omega)$ has two δ-functional peaks at $\omega = E_k^c$ and E_k^v, and the density of states has a gap $2\Delta_0 = U$. Our goal is to analyze how this spectral function gets modified once we use Eq. (4) and compute thermal fermionic self-energy and thermal corrections to $\langle S_z \rangle$.

A. One-loop perturbation theory

There are several contributions to fermionic self-energy $\Sigma(k,\omega)$ to one loop order, but the earlier study by Morr and one of us has found[21] that the dominant one at the lowest T comes from the interaction between valence and conduction fermions mediated by the exchange of low-energy transverse spin waves (see Ref. 21 for details). To one-loop order, spin-wave-mediated interaction gives rise to

$$\Sigma_1^{v,c}(\omega,\mathbf{k}) = \beta\Delta_0^2 G_{c,v}(\omega,\mathbf{k}) = \frac{\beta\Delta_0^2}{\omega - \bar{E}_k^{cv}}, \tag{7}$$

where, we remind, $\beta = (T/\pi J)|\log \epsilon|$. The order parameter also acquires a correction proportional to β. To obtain it, one has to substitute the self-energy into the Green's function and compute $\langle S_z \rangle$ using Eq. (3), but with the full G instead of G_0. This yields

$$\langle S_z \rangle = \frac{1}{2}\left(1 - \frac{\beta}{2}\right), \tag{8}$$

i.e., $\Delta^2 = \Delta_0^2[1 - \beta + O(\beta^2)]$. The $O(\beta)$ ($|\log \epsilon|$) correction to $\langle S_z \rangle$ is in agreement with Mermin-Wagner theorem. However, when we combine self-energies Eq. (7) and $G_0^{v,c}$ in which $\Delta_0 = U/2$ is replaced by $\Delta = U\langle S_z \rangle$ and obtain the new Green's function, we find that $O(\beta)$ terms cancel out, i.e., to first order in β the fermionic Green's function does not change
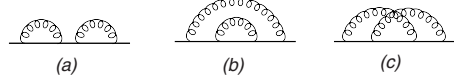

(a)   (b)   (c)

FIG. 3. Three equivalent diagrams for two-loop corrections to the Green's function. The second and the third diagrams contribute to fermionic self-energy.

$$G(\omega,k,\beta) \approx \frac{1}{2}\left[\frac{1}{\omega - E_c - \Sigma_1^c} + \frac{1}{\omega - E_v - \Sigma_1^v}\right]$$
$$= \frac{\bar{\omega}}{\bar{\omega}^2 - 16t^2\gamma_k^2 - (\Delta^2 + \beta\Delta_0^2)} = G_0(\omega,k), \tag{9}$$

where $\bar{\omega} = \omega + 4t' \cos k_x \cos k_y + \mu$. This result was obtained in Ref. 21 and was interpreted as an indication that the SDW form of $G(k,\omega)$ may survive even when $\langle S_z \rangle$ vanishes. However, one-loop result is at best indicative, and we need to go to higher orders to verify what happens with the fermionic Green's function when β increases.

B. Two-loop corrections

As the next step, we obtain two-loop formulas for the self-energy and $\langle S_z \rangle$. The two-loop diagrams for the self-energy are the second and third diagrams in Fig. 3. Evaluating them in the same approximation as one-loop diagram, we obtain

$$\Sigma_2^c(\omega,\mathbf{k}) = \frac{2\beta^2\Delta_0^4}{(\omega - E_k^v)(\omega - E_k^c)^2},$$

$$\Sigma_2^v(\omega,\mathbf{k}) = \frac{2\beta^2\Delta_0^4}{(\omega - E_k^v)^2(\omega - E_k^c)}. \tag{10}$$

Substituting these self-energies into the valence and conduction Green's functions together with one-loop diagrams, we obtain after a simple algebra

$$G(\omega,\mathbf{k}) = \frac{\bar{\omega}}{3}\left[\frac{2}{\bar{\omega}^2 - 16t^2\gamma_k^2 - (\Delta^2 + 2\Delta_0^2\beta)} + \frac{1}{\bar{\omega}^2 - 16t^2\gamma_k^2 - (\Delta^2 - \Delta_0^2\beta)}\right]. \tag{11}$$

Evaluating $\langle S_z \rangle$ in the same two-loop approximation we obtain

$$\langle S_z \rangle = \frac{1}{2}\left(1 - \frac{\beta}{2} + \frac{5\beta^2}{8}\right), \tag{12}$$

such that $\Delta^2 = \Delta_0^2[1 - \beta + 3\beta^2/2 + O(\beta^3)]$. Substituting now this Δ^2 into Eq. (11) we find that, up to two-loop order,

$$G(\omega,\mathbf{k}) = \frac{\bar{\omega}}{3}\left[\frac{2}{\bar{\omega}^2 - 16t^2\gamma_k^2 - \Delta_1^2} + \frac{1}{\bar{\omega}^2 - 16t^2\gamma_k^2 - \Delta_2^2}\right], \tag{13}$$

where $\Delta_1 = \Delta_0(1 + \beta/2 + 5\beta^2/8)$ and $\Delta_2 = \Delta_0(1 - \beta + \beta^2/4)$.

We see that the Green's function splits into two components. Both have SDW form, but the values of Δ are different
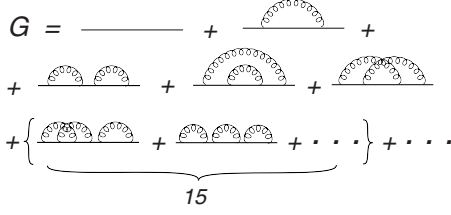
FIG. 4. Diagrammatic series for the Green's function. Only thermal contributions in which a fermion jumps from a valence to a conduction band (and vice versa) and emits (absorbs) a transverse spin wave are included.

$-\Delta_2$ decreases with β while Δ_1 increases. This implies that the peak in the spectral function, originally located at $\bar{\omega}^2 = 16t^2\gamma_k^2 + \Delta_0^2$, splits into two subpeaks—one shifts to higher $|\bar{\omega}|$, another to smaller $|\bar{\omega}|$. This is the new trend, not present in the one-loop approximation.

This consideration also shows that to understand what happens when $\beta = O(1)$, one cannot restrict with a few first orders in the loop expansion but rather has to sum up infinite number of terms. This is what we are going to do next.

C. Nonperturbative Green's function

We list several results which can be explicitly verified by doing loop-expansion order by order in β. (1) The SDW order parameter $\langle S_z \rangle$ is given by the same loop expression as in the mean-field theory, Eq. (3), but with the full G instead of G_0. (2) The renormalized $\langle S_z \rangle$, in turn, appears in the Green's function through $G_0^{v,c}$ in which $\Delta_0 = U/2$ has to be replaced by $\Delta = U\langle S_z \rangle$. (3) The full Green's function $G(\omega, \mathbf{k}, \beta)$ is given by $G(\omega, \mathbf{k}, \beta) = v_k^2 G^v(\omega, \mathbf{k}, \beta) + u_k^2 G^c(\omega, \mathbf{k}, \beta)$, where $G^{v,c}$ are the full Green's functions for valence and conduction fermions and u_k and v_k are the same as in Eq. (1) but with Δ instead of Δ_0. (4) At loop order n of the perturbation theory there are $(2n-1)!!$ equivalent contributions to the full $G^{c,v}$, each contains $[\beta G_0^v(\omega, \mathbf{k}) G_0^c(\omega, \mathbf{k})]^n$ (see Fig. 4).

Because of the last item, it is advantageous to sum up infinite series of diagrams for the Green's function rather than for the self-energy. We have

$$G_{tr}^{v,c}(\omega, \mathbf{k}, \beta) = G_0^{v,c}(\omega, \mathbf{k}) + \sum_{n=1}^{\infty} (2n-1)!! G_0^{v,c}(\omega, \mathbf{k})$$

$$\times [\beta \Delta_0^2 G_0^v(\omega, \mathbf{k}) G_0^c(\omega, \mathbf{k})]^n + \cdots, \quad (14)$$

where dots stand for nonlogarithmic corrections and subindex tr implies that we only considered interaction with transverse spin waves.

Substituting the expressions for $G_0^{v,c}$ and summing up asymptotic series we obtain

$$G_{tr}^{v,c}(\omega, \mathbf{k}, \beta) = \frac{2}{\Delta_0} \left(\frac{\pi}{2\beta} \right)^{1/2} \frac{\bar{\omega} \mp E_k}{(\bar{\omega}^2 - E_k^2)^{1/2}} \exp\left\{ -\frac{\bar{\omega}^2 - E_k^2}{2\Delta_0^2 \beta} \right\}$$

$$\left\{ i + \text{Erfi}\left[\sqrt{\frac{\bar{\omega}^2 - E_k^2}{2\Delta_0^2 \beta}} \right] \right\} + \cdots, \quad (15)$$

where $\text{Erfi}(z) = -i\,\text{Erf}(iz)$ is imaginary error function [$\text{Erfi}(x)$

is real when x is real and imaginary when x is imaginary]. Observe that $\text{Im}\,G_{tr}^{v,c}$ vanishes when $\bar{\omega}^2 < E_k^2$.

To one-loop order, Eq. (15) reduces to $G_0^{v,c}$, but beyond one loop the Green's functions $G^{v,c}$ obviously become β dependent. The spectral function $A_{tr}(\omega, \mathbf{k}, \beta) = \pi^{-1}|\text{Im}\,G(\omega - i0, \mathbf{k}, \beta)|$ is readily obtained from Eq. (15)

$$A_{tr}(\omega, \mathbf{k}, \beta) = \frac{2}{\Delta_0} \sqrt{\frac{1}{2\pi\beta}} e^{-(\bar{\omega}^2 - E_k^2)/2\Delta_0^2 \beta}$$

$$\times \frac{u_k^2|\bar{\omega} + E_k| + v_k^2|\bar{\omega} - E_k|}{(\bar{\omega}^2 - E_k^2)^{1/2}} \theta[\bar{\omega}^2 - E_k^2], \quad (16)$$

where $\theta(x) = 1$ for $x > 0$ and zero otherwise.

Substituting $G^{v,c}$ from Eq. (15) into the expression for $\langle S_z \rangle$ we obtain how the SDW order parameter evolves with β

$$\langle S_z \rangle = \frac{1}{2} \int \frac{d^2k}{(2\pi)^2} \sqrt{\frac{2}{\pi\beta}} \frac{\Delta}{\Delta_0} \int_{-\infty}^{\infty} d\bar{\omega} \frac{\exp\left\{ -\frac{\bar{\omega}^2 - E_k^2}{2\Delta_0^2 \beta} \right\}}{\sqrt{\bar{\omega}^2 - E_k^2}}$$

$$\times n_F(\bar{\omega} - \mu - 4t'\cos k_x \cos k_y) \theta[\bar{\omega}^2 - E_k^2]. \quad (17)$$

The remaining unknown parameter μ is fixed by the condition on the number of particles in the SDW state[60]

$$\frac{(1-x)}{2} = \int \frac{d^2k\,d\omega}{(2\pi)^2} A_{tr}(\omega, \mathbf{k}, \beta) n_F(\omega). \quad (18)$$

These coupled equations were solved numerically. The dependence of $\langle S_z \rangle$ on β or doping x is quite as expected: $\langle S_z \rangle$ monotonically decreases as β or x increase, and vanishes at some particular β_{cr} and x_{cr} (see Fig. 6). The spectral function $A_{tr}(\omega, \mathbf{k}, \beta)$ has sharp δ-functional peaks at $\beta \to 0$, at $\bar{\omega} = \pm E_k$ ($\omega = E_k^{v,c}$). At finite β, quasiparticle peaks transform into branch cuts at $|\bar{\omega}| = E_k$, with the width of order $\beta \propto T$, and the spectral weight extends to larger frequencies. Near the branch cut $A_{tr}(\omega, \mathbf{k}, \beta)$ diverges as $1/\sqrt{x}$. We plot $A_{tr}(\omega, \mathbf{k}, \beta)$ at a hot spot $\mathbf{k}_{hs} = (k_x, \pi - k_x)$ in Fig. 5.

D. Further modifications of the spectral function

On a more careful look, we found that the spectral function given by Eq. (16) have to be further modified by two reasons. First, in the calculations above we only included the self-energy due to exchange of transverse spin waves, and neglected the self-energy due to exchange of longitudinal spin fluctuations. This is justified at small β, when longitudinal fluctuations are gapped, but when $\beta \approx \beta_{cr}$, longitudinal fluctuations are nearly gapless and are as important as transverse ones. The limiting case when transverse and longitudinal spin propagators are identical can be studied within the same approximation as before, the only difference is that combinatoric factors are now $(2n+1)!!/2^n$ (Ref. 22). As a result, the spectral function becomes
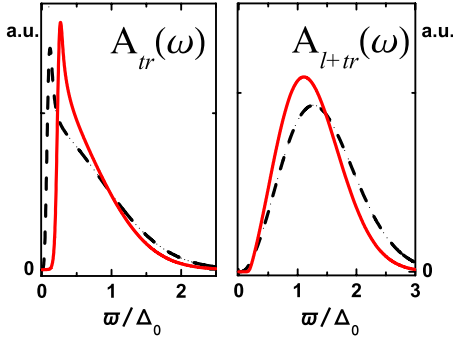
FIG. 5. (Color online) The spectral function $A(\omega, k_{hs}, \beta)$ at a hot spot. Here and below a.u. stand for arbitary units. Left panel $-A_{tr}$, obtained by including only transverse spin waves. Right panel $-A_{l+tr}$, obtained by treating transverse and longitudinal spin excitations on equal footings. Dashed lines $-\beta = 0.6\beta_{cr}$, solid lines $-\beta = 0.8\beta_{cr}$. A_{tr} has a branch cut at energy which scales with the magnitude of SDW order parameter, while A_{l+tr} has a hump at energy which roughly remains the same as SDW gap at $T = 0$. The actual $A(\omega, k_{hs}, \beta)$ at $\beta < \beta_{cr}$ coincides with A_{tr} at low frequencies, and crosses over to A_{l+tr} at frequencies larger than the gap for longitudinal fluctuations. As a result, the actual spectral function has a peak at a low energy and a hump at a higher energy.

$$A_{l+tr}(\omega, \mathbf{k}, \beta) = \frac{1}{\Delta_0^3} \frac{4}{\sqrt{\pi \beta^3}} \exp\left\{ \frac{-(\bar{\omega}^2 - E_k^2)}{\Delta_0^2 \beta} \right\}$$

$$\times \frac{u_k^2 |\bar{\omega} + E_k| + v_k^2 |\bar{\omega} - E_k|}{(\bar{\omega}^2 - E_k^2)^{-1/2}} \theta[\bar{\omega}^2 - E_k^2],$$

$$(19)$$

where subindex $l+tr$ implies that this is a contribution from both longitudinal and transverse spin excitations. One can easily make sure that A_{l+tr} is also fully incoherent at $\beta > 0$, but, in distinction to A_{tr}, it vanishes at $\bar{\omega} = \pm E_k$ and has a hump at a frequency which remains of order Δ_0 for all $\beta < \beta_{cr}$. We plot $A_{l+tr}(\omega, \mathbf{k}, \beta)$ at a hot spot in Fig. 5. The function $A_{l+tr}(\omega, \mathbf{k}_{hs}, \beta)$ becomes particularly simple at $\beta \geq \beta_{cr}$

$$A_{l+tr}(\omega, \mathbf{k}_{hs}) = \frac{\omega^2}{\Delta_0} \frac{4}{\sqrt{\pi \beta^3}} \exp\left\{ -\frac{\omega^2}{\beta \Delta_0^2} \right\}. \qquad (20)$$

For a generic $\beta \lesssim \beta_{cr}$, Eq. (19) is the correct result at high energies, larger than the longitudinal gap and Eq. (16) is the correct result at smaller energies. As β approaches β_{cr} the range of applicability of $A_{tr}(\omega, \mathbf{k}_{hs})$ shrinks. The full formula cannot be obtained within eikonal approximation, but it is clear that the actual $A(\omega, \mathbf{k}, \beta)$ contains both the branch cut, $1/\sqrt{x}$ singularity near $\omega = E_k^{v,c}$ and the hump at a frequency of order Δ_0, where the quasiparticle peaks were located at $\beta = 0$. To simplify the computational procedure, in Fig. 9 below we use for the actual $A(\omega, \mathbf{k}_{hs}, \beta)$ the function $A_{tr}(\omega, \mathbf{k}_{hs}, \beta)$ up to a frequency where it crosses with A_{l+tr}, and use the function $A_{l+tr}(\omega, \mathbf{k}_{hs}, \beta)$ at larger frequencies.

Second, Eqs. (16) and (19) show that fermionic coherence is lost immediately when β becomes nonzero (the pole transforms into a branch cut). Meanwhile, from physics perspective, as long as the system has an SDW order, a Fermi-liquid
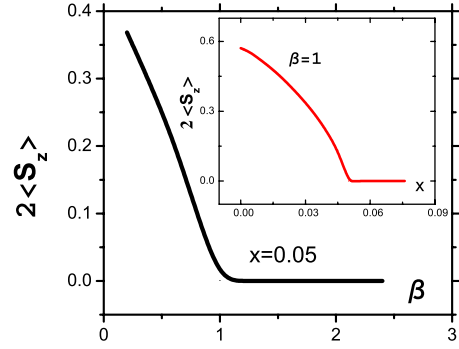

FIG. 6. (Color online) The SDW order parameter $\langle S_z \rangle$ vs β at a given $x = 0.05$. For simplicity, we set Z_β to be a constant (=0.2). Inset: $\langle S_z \rangle$ vs x at a given $\beta = 1$.

behavior near the pocketed FS should be preserved, i.e., a quasiparticle peak with $T^2 \log T$ width should survive, albeit with a reduced magnitude. The reason it was lost in the calculations above is because we completely neglected regular classical and quantum corrections to the Green's function [dots in Eq. (14)]. We verified that, when these terms are included, only a part of $G_0^{v,c}$ gets involved in the renormalizations by series of β^n corrections, the other stays intact. This implies that the actual $A_{full}^{v,c} = Z_\beta A_0^{v,c} + (1 - Z_\beta) A^{v,c}$. The residue Z_β is some number $0 < Z_\beta < 1$ at $\beta = 0$, where anyway $A^{v,c} = A_0^{v,c}$, it decreases as β increases and vanishes at $\beta = \beta_{cr}$. For definiteness, we used $Z_\beta = 0.2$ in the panel $0 < \beta < \beta_{cr}$ in Figs. 8 and 9.

These two additions also affect the formula for $\langle S_z \rangle$ and the equation for μ, which become

$$\langle S_z \rangle = Z_\beta \int \frac{d^2 k}{(2\pi)^2} \frac{\Delta}{E_k} [n_F(E_k^v) - n_F(E_k^c)]$$

$$+ (1 - Z_\beta) \frac{1}{2} \int \frac{d^2 k}{(2\pi)^2} \sqrt{\frac{2}{\pi \beta}} \frac{\Delta}{\Delta_0}$$

$$\int_{-\infty}^{\infty} d\bar{\omega} \frac{\exp\left\{ -\frac{\bar{\omega}^2 - E_k^2}{2\Delta_0^2 \beta} \right\}}{\sqrt{\bar{\omega}^2 - E_k^2}}$$

$$n_F(\bar{\omega} - \mu - 4t' \cos k_x \cos k_y) \theta[\bar{\omega}^2 - E_k^2] \qquad (21)$$

and

$$\frac{(1-x)}{2} = \int_{-\infty}^{\infty} d\omega \int \frac{d^2 k}{(2\pi)^2} n_F(\omega) \left\{ \frac{Z_\beta}{\pi} [v_k^2 \delta(\omega - E_k^v) \right.$$

$$\left. + u_k^2 \delta(\omega - E_k^c)] + (1 - Z_\beta) A(\omega, \mathbf{k}) \right\}. \qquad (22)$$

III. RESULTS

We solved Eqs. (21) and (22) numerically and plot the dependence of the order parameter $\langle S_z \rangle$ on β and x in Fig. 6. We used several phenomenological forms of Z_β in which $Z_{\beta_{cr}} = 0$, but found that the functional forms of the spectral functions do not depend on Z_β in any substantial way. For
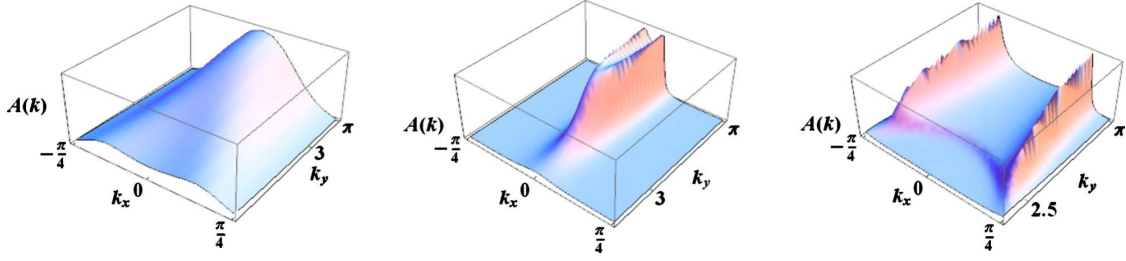
FIG. 7. (Color online) The appearance and evolution of the electron pocket near $(k_x, k_y) = (0, \pi)$ and symmetry related points. Electron pocket appears as a single point at $(0, \pi)$ once β increases and reaches a critical value, and evolves with increasing β. From left to right: $\beta/\beta_{cr} = 0.8; 0.85; 0.95$. We set $x = 0.02$.

simplicity, and because below we only present the results for a few β in the SDW state, we set $Z_\beta = 0.2$, independent of the actual β. Also, all cases (even when $Z_\beta = 0$) $\langle S_z \rangle$ monotonically decreases when either x or β increase and vanishes at some x_{cr} and β_{cr}.

In Fig. 7 we show the evolution of the electron Fermi surface near $(0, \pi)$ and symmetry-related points. The electron pocket is absent at small β, when SDW order is strong, but appears when β exceeds some critical value. The electron pocket evolves with increasing β and eventually disappears when the system looses long-range SDW order. This behavior is qualitatively consistent with the mean-field SDW picture.

The results for $A_{full}(\omega, k, \beta)$ are presented in Figs. 8–10. In Fig. 8 we plot the full spectral function at zero frequency along the diagonal direction in the Brillouin zone. In the two limits, $\beta = 0$ and $\beta \gg \beta_{cr}$, the system possesses sharp quasiparticles—in the first case at the two sides of the hole

pocket, in the second case at the large, Luttinger FS. In between, the spectral function evolves, as β increases, from a well-pronounced two-peak structure to a completely incoherent structure at $\beta = \beta_{cr}$, in which the spectral weight at $\omega = 0$ is spreaded between the original and the shadow FSs [in reality, $A_{full}(0, k, \beta)$ spreads outside of this range, but to find these tails of the spectral function one has to go beyond the accuracy of our calculations]. This result implies that the system does retain some memory about SDW pockets even when $\beta = \beta_{cr}$ and $\Delta = 0$. When β becomes larger than β_{cr} and SDW order disappears, the region where $A_{full}(0, k, \beta) \neq 0$ progressively shrinks with increasing β toward a single quasiparticle peak. We emphasize that this evolution of $A_{full}(0, k, \beta)$ with β is very different from that in the mean-field SDW theory, where the spectral function in the SDW state has two peaks at the two sides of the hole pocket and the shadow peak just disappears when Δ vanishes.
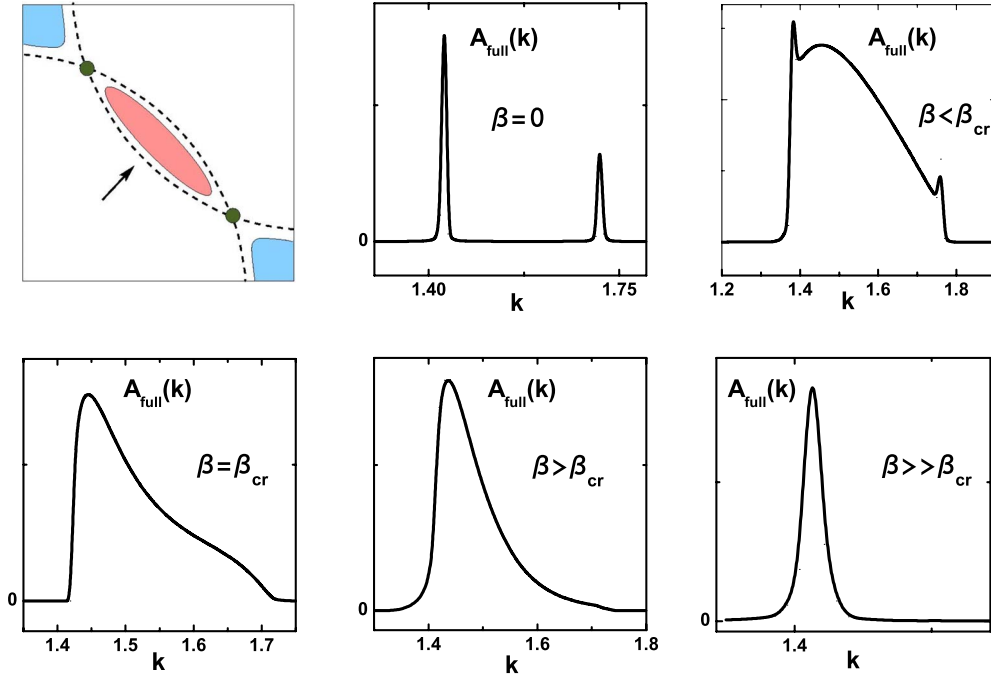

FIG. 8. (Color online) The spectral function, $A_{full}(\omega, \mathbf{k}, \beta)$ at $\omega = 0$ along the diagonal (nodal) direction in the Brillouin zone. We used $Z = 0.2$ for the top right panel. Observe that the systems retains a memory about a shadow FS when SDW order disappears at $\beta = \beta_{cr}$ (the spectral weight is nonzero in the whole region between the original and the shadow FSs). We set $x = 0.05$, $t = 0.32\Delta_0$, $t' = -0.2t$. For these parameters, $\beta_{cr} \approx 1$.
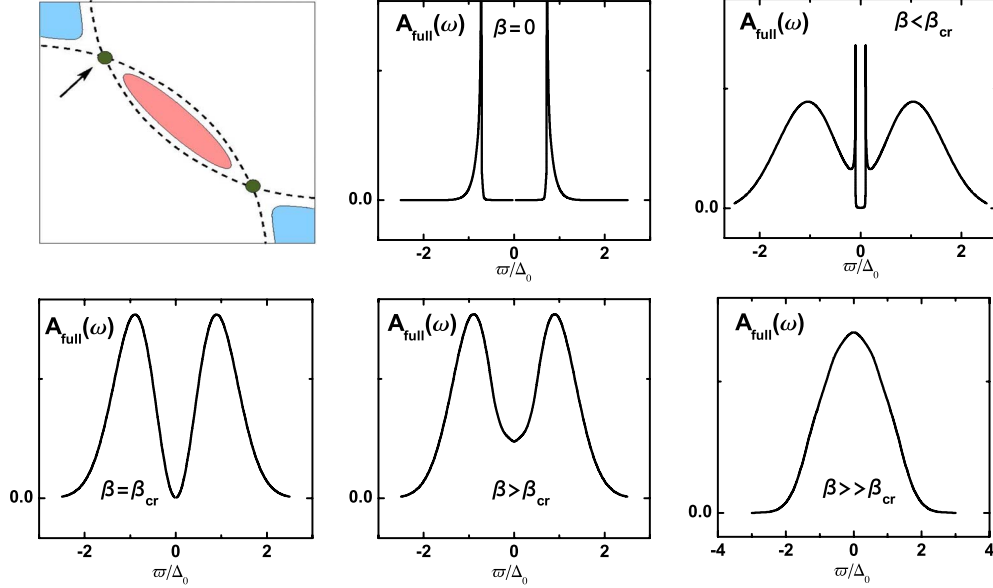
FIG. 9. (Color online) The spectral function $A_{full}(\omega, \mathbf{k}_{hs}, \beta)$ at a hot spot, at various β. The frequency is in units $\bar{\omega}/\Delta_0$, where $\bar{\omega} = \omega + \mu - 4t' \cos^2 k_x$. The parameters are the same as in Fig. 8.

In Fig. 9 we show the frequency dependence of $A_{full}(\omega, k_{hs}, \beta)$ at a hot spot for a wide range of β. In the two limits, the behavior is again coherent: there are quasiparticle peaks at $\bar{\omega} = \omega + \mu - 4t' \cos^2 k_x = \pm \Delta_0$ deep in the SDW phase, and the peak centered at $\bar{\omega} = \omega = 0$ deep in the normal phase. In between, the spectral function is again predominantly incoherent. Specifically, as β increases toward β_{cr}, the quasiparticle peak splits into the peak at $\bar{\omega} = \Delta$, and the hump at a larger frequency. The frequency where the peak is located shifts downwards with decreasing β, while the hump remains roughly at around Δ_0, and, on a more careful look, shifts toward somewhat larger frequency. We show this behavior in more detail in Fig. 10, where we plot the spectral function for a range of $\beta < \beta_{cr}$. The peak in the spectral function is the property of A_{tr} and A_0 and the hump is the property of A_{l+tr}. We emphasize that the peak and the hump

do coexist in the SDW phase, the first describes coherent low-energy excitations, the second describes fully incoherent high-energy excitations. Once SDW order disappears at β_{cr}, coherent excitations also disappear, but the hump remains and disappears only at much larger β. It is quite natural to identify the hump at $\beta > \beta_{cr}$ with the pseudogap, and low-energy coherent excitations existing at $\beta < \beta_{cr}$ with the building blocks for magneto-oscillations. The implication of this result is that the 200 meV pseudogap observed in ARPES in zero field[13] *is not* an obstacle for observing magneto-oscillations once the system becomes SDW ordered.

A. Density of states

The density of states (DOS) in the SDW phase, $N(\omega, \beta) = \int (d^2k/4\pi^2) A(\omega, \mathbf{k}, \beta)$, is obtained from Eqs. (1), (16), and (19). The expressions for $N(\omega)$ at finite β are rather complex for $t' \neq 0$ but are simplified for $t' = 0$ which we assume to hold in this section. A finite t' affects the behavior of the DOS at the smallest frequencies, but not at frequencies $\omega + \mu \gtrsim \Delta$, which we are chiefly interested in.
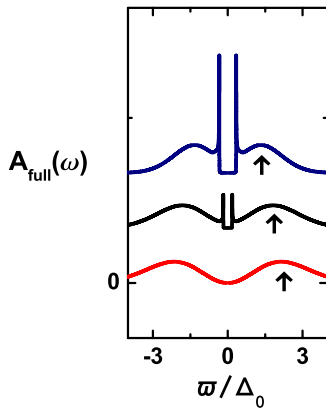
For free fermions, we then have

FIG. 10. (Color online) The spectral function $A_{full}(\omega, \mathbf{k}_{hs}, \beta)$ at a hot spot, at various $0 < \beta \leq \beta_{cr}$. The lowest plot corresponds to $\beta = \beta_{cr}$, values of β decrease from bottom up. The frequency is in units $\bar{\omega}/\Delta_0$. The parameters are the same as in Fig. 8. As β decreases, the peak and the hump come closer to each other.

$$N_0(\omega, \beta) = \frac{\bar{\omega}}{\pi^2} \int \int_{-1}^{1} \frac{dudv}{\sqrt{1-u^2}\sqrt{1-v^2}} \delta[\bar{\omega}^2 - \Delta^2 - 4t^2(u+v)^2]$$

$$= \frac{1}{2\pi^2 t} \frac{\bar{\omega}}{\sqrt{\bar{\omega}^2 - \Delta^2}} K\left[\sqrt{1 - \frac{\bar{\omega}^2 - \Delta^2}{16t^2}}\right], \qquad (23)$$

where $K(x)$ is the complete elliptic integral of the first kind (defined as in Ref. 61), and for $t' = 0$, $\bar{\omega} = \omega + \mu$. The DOS vanishes at $|\bar{\omega}| < \Delta$, diverges as $1/\sqrt{x}$ at $|\bar{\omega}| = \Delta + 0$, monotonically decreases at larger frequencies, and <u>discontinuously drops to zero at the bandwidth, when $|\bar{\omega}| = \sqrt{\Delta^2 + 16t^2}$.</u>

The DOS $N_{tr}(\omega, \beta)$ obtained using the spectral function A_{tr} from Eq. (16) reduces to a 1D integral

$$N_{tr}(\omega, \beta) = \frac{\bar{\omega}}{2\pi^{5/2}t} \int_0^{\sqrt{(\bar{\omega}^2 - \Delta^2)/2\beta\Delta_0^2}} \frac{dze^{-z^2}}{\sqrt{\bar{\omega}^2 - \Delta^2 - 2\beta\Delta_0^2 z^2}}$$
$$\times K\left[\sqrt{1 - \frac{\bar{\omega}^2 - \Delta^2 - 2\beta\Delta_0^2 z^2}{16t^2}}\right] \quad (24)$$

for $0 < \bar{\omega}^2 - \Delta^2 < 16t^2$ and

$$N_{tr}(\omega, \beta) = \frac{\bar{\omega}}{2\pi^{5/2}t} \int_{\sqrt{(\bar{\omega}^2 - \Delta^2 - 16t^2)/2\beta\Delta_0^2}}^{\sqrt{(\bar{\omega}^2 - \Delta^2)/2\beta\Delta_0^2}} \frac{dze^{-z^2}}{\sqrt{\bar{\omega}^2 - \Delta^2 - 2\beta\Delta_0^2 z^2}}$$
$$\times K\left[\sqrt{1 - \frac{\bar{\omega}^2 - \Delta^2 - 2\beta\Delta_0^2 z^2}{16t^2}}\right] \quad (25)$$

for $\bar{\omega}^2 - \Delta^2 > 16t^2$. [The trick how to integrate over 2D momenta k_x and k_y in $\int d^2k/(4\pi^2) A_{tr}(\omega, \mathbf{k}, \beta)$ is to introduce $u = \cos k_x$ and $v = \cos k_y$ as new variables, use the identity

$$\frac{e^{-(\bar{\omega}^2 - E_k^2)/2\beta\Delta_0^2}}{\sqrt{\bar{\omega}^2 - E_k^2}} 2\sqrt{2\beta\Delta_0^2} = \int_0^\infty dze^{-z^2} \delta(\bar{\omega}^2 - E_k^2 - 2\beta\Delta_0^2 z^2)$$

$$(26)$$

and use δ function to perform the momentum integration]. The density of states N_{tr} vanishes at $|\bar{\omega}| < \Delta$, diverges logarithmically at $|\bar{\omega}| = \Delta + 0$, and monotonically decreases at larger frequencies. There is no threshold at the bandwidth as $A_{tr}(\omega, \mathbf{k}, \beta)$ is nonzero everywhere at $|\bar{\omega}| > \Delta$, but, indeed, at frequencies larger than the bandwidth our approximation eventually breaks down.

For the spectral function A_{l+tr} from Eq. (19), we obtain, using the same trick,

$$N_{l+tr}(\omega, \beta) = \frac{\bar{\omega}}{\pi^{5/2}t} \int_0^{\sqrt{(\bar{\omega}^2 - \Delta^2)/\beta\Delta_0^2}} \frac{dzz^2 e^{-z^2}}{\sqrt{\bar{\omega}^2 - \Delta^2 - \beta\Delta_0^2 z^2}}$$
$$\times K\left[\sqrt{1 - \frac{\bar{\omega}^2 - \Delta^2 - \beta\Delta_0^2 z^2}{16t^2}}\right] \quad (27)$$

for $0 < \bar{\omega}^2 - \Delta^2 < 16t^2$ and

$$N_{l+tr}(\omega, \beta) = \frac{\bar{\omega}}{\pi^{5/2}t} \int_{\sqrt{(\bar{\omega}^2 - \Delta^2 - 16t^2)/\beta\Delta_0^2}}^{\sqrt{(\bar{\omega}^2 - \Delta^2)/\beta\Delta_0^2}} \frac{dzz^2 e^{-z^2}}{\sqrt{\bar{\omega}^2 - \Delta^2 - \beta\Delta_0^2 z^2}}$$
$$\times K\left[\sqrt{1 - \frac{\bar{\omega}^2 - \Delta^2 - \beta\Delta_0^2 z^2}{16t^2}}\right] \quad (28)$$

for $\bar{\omega}^2 - \Delta^2 > 16t^2$. This spectral function is continuous at $|\bar{\omega}| = \Delta$ and has a broad maximum at frequencies comparable to Δ_0.

This behavior is very similar to the one for the spectral function. Again, the transverse-only contribution N_{tr} has a peak at the frequency $\bar{\omega} = \Delta$, which scales with the order parameter of the SDW phase, while N_{l+tr} which treats contributions from transverse and longitudinal fluctuations on equal footings (as if longitudinal excitations were massless) has no features at Δ, but has a broad maximum at a frequency which remains comparable to Δ_0. Just like the spectral function, the actual DOS $N(\omega, \beta)$ interpolates between these two terms. At frequencies smaller than the gap for longitudinal spin excitations, $N(\omega, \beta) \approx N_{tr}(\omega, \beta)$, while at
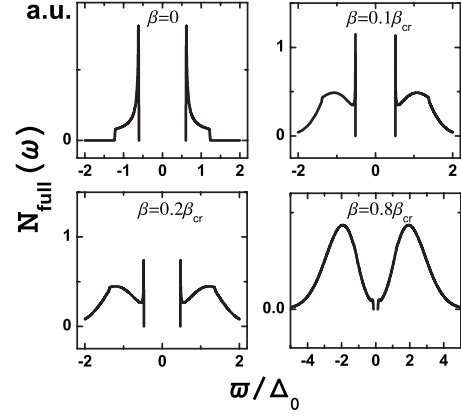

FIG. 11. Density of states vs $\bar{\omega}/\Delta_0$ for different values of β. We set $t' = 0$ and $t = 0.32\Delta_0$.

larger frequencies $N(\omega, \beta)$ gradually approaches $N_{l+tr}(\omega, \beta)$.

We plot the DOS in Fig. 11. We again set $N(\omega, \beta) = N_{tr}(\omega, \beta)$ at frequencies smaller than the crossing point between $N_{tr}(\omega, \beta)$ and $N_{l+tr}(\omega, \beta)$, and set $N(\omega, \beta) = N_{l+tr}(\omega, \beta)$ at higher frequencies. And we again assumed that the full DOS $N_{full}(\omega, \beta)$ is the sum of the incoherent $N(\omega, \beta)$ with the factor $1 - Z_\beta$ and the coherent, mean-field $N_0(\omega, \beta)$ with the factor Z_β.

The plots clearly show the same trends in the DOS as we just discussed. At small β, there is a sharp gap $2\Delta_0 \approx U$ between valence and conduction bands. As β increases, sharp gap decreases, the spectral weight extends to higher frequencies, and the DOS develops a hump at an energy comparable to Δ_0 (i.e., the distance between the humps remains U). The peak in the DOS at the boundary of the sharp gap gets smaller as β increases and the sharp gap decreases. At $\beta = \beta_{cr}$ the gap and the peak disappear, and the spectral function only possesses a hump. As β increases even further, the DOS at $\bar{\omega} = 0$ increases (and also μ gets reduced such that $\bar{\omega}$ comes closer to ω), and eventually the DOS at low frequencies recovers weakly frequency-dependent form of a metal with a large FS.

This physics is somewhat spoiled in the plots of $N_{full}(\omega, \beta)$ by the change in the behavior of $N_{tr+l}(\omega, \beta)$ at the bandwidth (at $\bar{\omega} = \sqrt{\Delta^2 + 16t^2}$). This change in behavior is seen in Fig. 11 as the discontinuity in the frequency derivative of $N_{full}(\omega, \beta)$. For large β the hump in the DOS is predominantly the effect of the bandwidth. However, at intermediate β, the hump is located at a frequency below the bandwidth, as is clearly visible in the top right panel of Fig. 11 ($\beta = 0.1\beta_{cr}$) and is therefore due to the physics that we described above.

B. Optical conductivity

The peak/hump structure also shows up in the optical conductivity. We computed the conductivity by standard means: by convoluting two full spectral functions A_{full} using Kubo formula
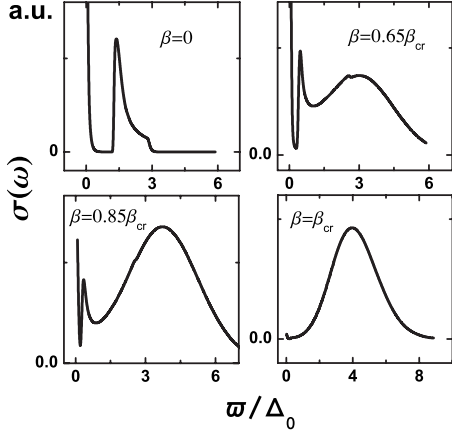
FIG. 12. Optical conductivity, $\sigma(\omega)$, for different β in the SDW phase at $x=0.02$. For simplicity, we used $Z_\beta=0.12$ in all plots. At $\beta=0$ $\sigma(\omega)$ has a true gap and discontinuity at the onset of scattering between conduction and valence bands. The onset frequency is at $\bar{\omega}$ slightly smaller than $2\Delta_0=U$ because x is nonzero and the actual gap $\Delta < \Delta_0$. At finite β the discontinuity splits into a hump which slowly moves to a higher frequency and a peak which moves to a smaller energy. We verified that the peak position scales with $\langle S_z \rangle$.

$$\sigma(\omega) = \pi e^2 \int \frac{d^2 k}{(2\pi)^2} v_k^2 \int d\Omega$$
$$\frac{n_F(\Omega) - n_F(\Omega + \omega)}{\omega} A_{full}(\Omega, \mathbf{k}, \beta) A_{full}(\Omega + \omega, \mathbf{k}, \beta),$$

(29)

where v_k is fermionic velocity. We used the same computational procedure as before: combined mean-field contribution to A, with the prefactor Z_β, and incoherent part of A with the prefactor $1-Z_\beta$, and used A_{tr} for the incoherent part at small frequencies and A_{l+tr} at high frequencies. The results are shown in Fig. 12. We again set $t'=0$ to simplify the calculations. At small β, the conductivity almost vanishes up to $\bar{\omega} = 2\Delta_0 = U$. When β gets larger, the discontinuity at U splits into a hump which slowly shifts to a larger energy and a peak which scales with Δ and shifts to a smaller frequency as SDW order gets weaker. In addition, there also appears a Drude component at the smallest frequencies.

The hump at large $\beta \gtrsim \beta_{cr}$ is predominantly the effect of the bandwidth. It appears quite "sharp" in the last panel in Fig. 12, but this is the consequence of our approximation in which we neglected all regular self-energy terms. When these terms are included, the hump should definitely get broader.

This behavior of $\sigma(\omega)$ is quite consistent with the observed evolution of $\sigma(\omega)$ in the SDW phase of electron-doped $Nd_{2-x}Ce_xCuO_4$, where the region of SDW-ordered phase extends over a substantial doping range, up to $x \sim 0.15$. Onose et al.[45] and others[46] have found that conductivity does have a peak/hump structure at finite x, the hump shifts toward a higher frequency with increasing x (from a charge-transfer gap of 1.7 eV at $x=0$ to over 2 eV at $x=0.1$), while the peak shifts downwards as x increases and was

argued[46] to scale with the Neel temperature T_N. These two features are reproduced in our theory.

IV. CONCLUSIONS

To summarize, in this paper we obtained fermionic spectral function, the density of states, and optical conductivity in the SDW phase of the cuprates at small but finite T. We adopted nonperturbative approach and summed up infinite series of thermal self-energy terms, keeping at each order nearly divergent $T/J|\log \epsilon|$ terms, where ϵ is a deviation from a pure 2D, and neglecting regular T/J corrections. We found that, as SDW order decreases, the spectral function in the antinodal region acquires peak/hump structure: the peak position scales with the SDW order parameter, while the incoherent hump remains roughly at the same scale as at $T =0$, when SDW order is the strongest. We identified the hump with the pseudogap observed in ARPES experiments and identified coherent, Fermi-liquid excitations at low energies as building blocks for magneto-oscillations in an applied field. The same peak/hump structure appears in the DOS and in the optical conductivity. The gap in the DOS scales with the SDW order parameter and disappears when SDW order vanishes, however, the DOS also develops a hump at an energy which remains close to $U/2$, no matter what is value of the SDW order parameter. Optical conductivity at finite β has a Drude peak at the lowest frequencies, a peak, which again scales with the SDW order parameter and moves to smaller frequencies as β increases, and a hump which remains roughly omegaplus at U and slightly shifts to higher frequencies as SDW order gets weaker.

A more generic result of our study is the phase diagram for the cuprates shown in Fig. 1. A similar phase diagram has been proposed in Ref. 52. At large enough hole doping and small enough temperatures, thermal fluctuations are weak and no SDW precursors appear. In this region, FS is large and the physics is governed by the interaction between fermions and Landau-overdamped spin fluctuations. This interaction gives rise to a fermionic self-energy which is Fermi liquidlike at the lowest energies, has a non-Fermi-liquid form, $(i\omega)^a$, $a<1$ at high energies, and displays a marginal Fermi-liquid behavior in the crossover region.[7] The same interaction with overdamped spin fluctuations gives rise to a d-wave pairing instability.[8,9,48] The onset temperature for the d-wave pairing increases as x decreases and approaches the universal scale of around $T_p \sim 0.02 v_F/a$, where $v_F \sim 1$ eV$*a$ is the Fermi energy (Ref. 49). The actual superconducting T_c is lower due to fluctuations of the pairing gap. In this regime, the thermal evolution of the FS is entirely due to thermal effects associated s-wave fermionic damping induced by scattering on thermal bosons.[5,17] In particular, at a finite T, the spectral function is peaked at zero frequency in some range of k around the nodal direction, despite that the pairing gap itself has cos 2ϕ form.

At larger T and smaller $x>0$, thermal fluctuations get stronger and give rise to SDW precursors. These do not imply that the FS actually becomes pocketlike, but the spectral function in the antinodal region develops a hump at a finite frequency, and the low-energy spectral weight progressively

fills in the area between the actual FS at k_F and the shadow FS at $k=(\pi,\pi)-k_F$. This behavior is at least qualitatively consistent with recent ARPES experiments aimed to verify the existence of the outer side of a pocket.[62] We also emphasize that, as long as SDW order is weak, the incoherent pseudogap peak is the dominant feature in the ARPES spectrum. This last observation is particularly relevant to LBCO near 1/8 doping, for which there are indications of SDW ordering. This SDW order is in any case smaller than the order at half-filling, and it is very likely that the dominant ARPES intensity is remains the preudogap despite the potential appearance of SDW order. This would be consistent with the observations in Refs. 20 and 63.

The redistribution of the fermionic spectral weight, in turn, affects the pairing problem: in the presence of SDW precursors, T_c decreases with decreasing doping[51] because now the pairing is due to the exchange of propagating magnons rather than overdamped spin fluctuations, and the electron-magnon vertex gets smaller as SDW precursors get stronger.[21,53,54] A closely related effect which also reduces T-c is the removal of the low-energy spectral weight due to pseudogap opening.[64]

The precursors to SDW also give rise to domelike behavior of the onset temperature for the pairing in electron-doped cuprates (left-hand side of Fig. 1) but there the effect is weaker simply because pairing correlations are weaker.[47,65]

Recently we became aware of a study of thermal SDW fluctuations by Khodas and Tsvelik (Ref. 66). Their and our results are similar (e.g., both give linear in T width of the quasiparticle peaks at low T), but not identical as we studied isotropic quasi-2D systems with a true long-range SDW order below a certain small T ($\beta \le 1$) and exponential behavior of the correlation length at larger T, while Khodas and Tsvelik considered a 2D system with an easy-plane anisotropy and put special emphasis to the fact that spin correlations decay by a power law at small T.

[1] T. Timusk and B. Statt, Rep. Prog. Phys. **62**, 61 (1999); M. R. Norman, D. Pines, and C. Kallin, Adv. Phys. **54**, 715 (2005).

[2] K. K. Gomes, A. N. Pasupathy, A. Pushp, S. Ono, Y. Ando, and A. Yazdani, Nature (London) **447**, 569 (2007); A. Yazdani, J. Phys.: Condens. Matter **21**, 164214 (2009) and references therein.

[3] V. J. Emery and S. A. Kivelson, Nature (London) **374**, 434 (1995); I. Hetel, T. R. Lemberger, and M. Randeria, Nat. Phys. **3**, 700 (2007).

[4] B. Jankó, J. Maly, and K. Levin, Phys. Rev. B **56**, R11407 (1997); I. Kosztin, Q. Chen, B. Jankó, and K. Levin, ibid. **58**, R5936 (1998).

[5] M. Franz and A. J. Millis, Phys. Rev. B **58**, 14572 (1998).

[6] A. Paramekanti, M. Randeria, and N. Trivedi, Phys. Rev. B **70**, 054504 (2004).

[7] Ar. Abanov, A. V. Chubukov, and J. Schmalian, Adv. Phys. **52**, 119 (2003).

[8] D. J. Scalapino, Phys. Rep. **250**, 329 (1995); see also T. A. Maier, D. Poilblanc, and D. J. Scalapino, Phys. Rev. Lett. **100**, 237001 (2008).

[9] P. Monthoux and D. Pines, Phys. Rev. B **49**, 4261 (1994).

[10] See, e.g., T. Dahm, D. Manske, and L. Tewordt, Europhys. Lett. **55**, 93 (2001).

[11] B. Kyung, D. Senechal, and A.-M. S. Tremblay, Phys. Rev. B **80**, 205109 (2009).

[12] A. Kanigel, U. Chatterjee, M. Randeria, M. R. Norman, S. Souma, M. Shi, Z. Z. Li, H. Raffy, and J. C. Campuzano, Phys. Rev. Lett. **99**, 157001 (2007); A. Kanigel, M. R. Norman, M. Randeria, U. Chatterjee, S. Suoma, A. Kaminski, H. M. Fretwell, S. Rosenkranz, M. Shi, T. Sato, T. Takahashi, Z. Z. Li, H. Raffy, K. Kadowaki, D. Hinks, L. Ozyuzer, and J. C. Cam-puzano, Nat. Phys. **2**, 447 (2006).

[13] U. Chatterjee, M. Shi, D. Ai, J. Zhao, A. Kanigel, S. Rosenkranz, H. Raffy, Z. Li, K. Kadowaki, D. Hinks, Z. Xu, J. Wen, G. Gu, C. Lin, H. Claus, M. Norman, M. Randeria, and J. Campuzano, Nat. Phys. **6**, 99 (2010).; M. Shi, J. Chang, S. Pailhés, M. R. Norman, J. C. Campuzano, M. Månsson, T. Claesson, O. Tjernberg, A. Bendounan, L. Patthey, N. Momono, M. Oda, M. Ido, C. Mudry, and J. Mesot, Phys. Rev. Lett. **101**, 047002 (2008).

[14] K. Tanaka, W. S. Lee, D. H. Lu, A. Fujimori, T. Fujii, Risdiana, I. Tersaki, D. J. Scalapino, T. P. Devereaux, Z. Hussain, and Z-X. Shen, Science **314**, 1910 (2006).

[15] R. He, X. Zhou, M. Hashimoto, T. Yoshida, K. Tanaka, S. Mo, T. Sasagawa, N. Mannella, W. Meevasana, H. Yao, E. Berg, M. Fujita, T. Adachi, S. Komiya, S. Uchida, Y. Ando, F. Zhou, Z. Zhao, A. Fujimori, Y. Koike, K. Yamada, S. Kivelson, Z. Hussain, and Z. Shen, arXiv:0911.2245 (unpublished).

[16] For a discussion on this issue see, e.g., S. Hüfner, M. A. Hossain, A. Damascelli, and G. A. Sawatsky, Rep. Prog. Phys. **71**, 062501 (2008).

[17] M. R. Norman, M. Randeria, H. Ding, and J. C. Campuzano, Phys. Rev. B **57**, R11093 (1998); M. R. Norman, A. Kanigel, M. Randeria, U. Chatterjee, and J. C. Campuzano, ibid. **76**, 174501 (2007); A. V. Chubukov, M. R. Norman, A. J. Millis, and E. Abrahams, ibid. **76**, 180501(R) (2007); D. Wulin, C. Chien, D. Morr, and K. Levin, Phys. Rev. B **81**, 100504(R) (2010).

[18] T. Valla, A. V. Fedorov, J. Lee, J. C. Davis, and G. D. Gu, Science **314**, 1914 (2006); J. Meng, W. Zhang, G. Liu, L. Zhao, H. Liu, X. Jia, W. Lu, X. Dong, G. Wang, H. Zhang, Y. Zhou, Y. Zhu, X. Wang, Z. Zhao, Z. Xu, C. Chen, and X. J. Zhou, Phys. Rev. B **79**, 024514 (2009).

[19] A. Pushp, C. V. Parker, A. N. Pasupathy, K. K. Gomes, S. Ono, J. Wen, Z. Xu, G. Gu, and A. Yazdani, Science **324**, 1689 (2009); J. Lee, K. Fujita, A. R. Schmidt, C. K. Kim, H. Eisaki, S. Uchida, and J. C. Davis, *ibid.* **325**, 1099 (2009).

[20] R.-H. He, K. Tanaka, S.-K. Mo, T. Sasagawa, M. Fujita, T. Adachi, N. Mannella, K. Yamada, Y. Koike, Z. Hussain, and Z.-X. Shen, Nat. Phys. **5**, 119 (2009).

[21] A. V. Chubukov and D. K. Morr, Phys. Rep. **288**, 355 (1997).

[22] J. Schmalian, D. Pines, and B. Stojković, Phys. Rev. Lett. **80**, 3839 (1998); Phys. Rev. B **60**, 667 (1999); see also E. Z. Kuchinskii and M. V. Sadovskii, JETP **88**, 968 (1999).

[23] Y. M. Vilk and A.-M. S. Tremblay, J. Phys. I **7**, 1309 (1997).

[24] B. Kyung, S. Allen, and A.-M. S. Tremblay, Phys. Rev. B **64**, 075116 (2001); B. Kyung, V. Hankevych, A.-M. Dare, and A.-M. S. Tremblay, Phys. Rev. Lett. **93**, 147004 (2004); B. Kyung, S. S. Kancharla, D. Sénéchal, A.-M. S. Tremblay, M. Civelli, and G. Kotliar, Phys. Rev. B **73**, 165114 (2006).

[25] T. Das, R. S. Markiewicz, and A. Bansil, Phys. Rev. B **77**, 219904(E) (2008); R. S. Markiewicz, J. Lorenzana, G. Seibold, and A. Bansil, *ibid.* **81**, 014509 (2010).

[26] E. Z. Kuchinskii and M. V. Sadovskii, Pis'ma Zh. Eksp. Teor. Fiz. **88**, 224 (2008).

[27] K. Borejsza and N. Dupuis, Phys. Rev. B **69**, 085119 (2004).

[28] B. I. Shraiman and E. D. Siggia, Phys. Rev. B **46**, 8305 (1992).

[29] Y. M. Vilk and A.—M. S. Tremblay, J. Phys. Chem. Solids **56**, 1769 (1995); Europhys. Lett. **33**, 159 (1996); Y. M. Vilk, Phys. Rev. B **55**, 3870 (1997); G. Preosti, Y. M. Vilk, and M. R. Norman, Phys. Rev. B **59**, 1474 (2004).

[30] A. M. S. Tremblay, B. Kyung, and D. Senechal, Low Temp. Phys. **32**, 424 (2006).

[31] E. M. Motoyama, G. Yu, I. M. Vishik, O. P. Vajk, P. K. Mang, and M. Greven, Nature **445**, 186424 (2007).

[32] P. W. Anderson, Phys. Rev. Lett. **96**, 017001 (2006); P. A. Lee, N. Nagaosa, and X.-G. Wen, Rev. Mod. Phys. **78**, 17 (2006); S. Pathak, V. B. Shenoy, M. Randeria, and N. Trivedi, Phys. Rev. Lett. **102**, 027002 (2009).

[33] N. Doiron-Leyraud, C. Proust, D. LeBoeuf, J. Levallois, J.-B. Bonnemaison, R. Liang, D. A. Bonn, W. N. Hardy, and L. Taillefer, Nature (London) **447**, 565 (2007); D. LeBoeuf, N. Doiron-Leyraud, J. Levallois, R. Daou, J.-B. Bonnemaison, N. E. Hussey, L. Balicas, B. J. Ramshaw, R. Liang, D. A. Bonn, W. N. Hardy, S. Adachi, C. Proust, and L. Taillefer, *ibid.* **450**, 533 (2007); E. A. Yelland, J. Singleton, C. H. Mielke, N. Harrison, F. F. Balakirev, B. Dabrowski, and J. R. Cooper, Phys. Rev. Lett. **100**, 047003 (2008); A. F. Bangura, J. D. Fletcher, A. Carrington, J. Levallois, M. Nardone, B. Vignolle, P. J. Heard, N. Doiron-Leyraud, D. LeBoeuf, L. Taillefer, S. Adachi, C. Proust, and N. E. Hussey, *ibid.* **100**, 047004 (2008); C. Jaudet, D. Vignolles, A. Audouard, J. Levallois, D. LeBoeuf, N. Doiron-Leyraud, B. Vignolle, M. Nardone, A. Zitouni, R. Liang, D. A. Bonn, W. N. Hardy, L. Taillefer, and C. Proust, *ibid.* **100**, 187005 (2008); S. E. Sebastian, N. Harrison, E. Palm, T. P. Murphy, C. H. Mielke, R. Liang, D. A. Bonn, W. N. Hardy, and G. G. Lonzarich, Nature (London) **454**, 200 (2008); S. Sebastian, N. Harrison, C. Mielke, R. Liang, D. Bonn, W. Hardy, and G. Lonzarich, Phys. Rev. Lett. **103**, 256405 (2010); S. Sebastian, N. Harrison, M. Altarawneh, R. Liang, D. Bonn, W. Hardy, and G. Lonzarich, Phys. Rev. B **81**, 140505(R) (2010).

[34] Y. Zhang, E. Demler, and S. Sachdev, Phys. Rev. B **66**, 094501 (2002).

[35] D. Haug, V. Hinkov, A. Suchaneck, D. S. Inosov, N. B. Christensen, Ch. Niedermayer, P. Bourges, Y. Sidis, J. T. Park, A. Ivanov, C. T. Lin, J. Mesot, and B. Keimer, Phys. Rev. Lett. **103**, 017001 (2009).

[36] S. Chakravarty, R. B. Laughlin, D. K. Morr, and C. Nayak, Phys. Rev. B **63**, 094503 (2001).

[37] A. J. Millis and M. R. Norman, Phys. Rev. B **76**, 220503(R) (2007).

[38] M. Granath, Phys. Rev. B **77**, 165128 (2008).

[39] M. R. Norman (private communication).

[40] A.-M. Dare, Y. M. Vilk, and A.-M. S. Tremblay, Phys. Rev. B **53**, 014236 (1996).

[41] S. Chakravarty, B. I. Halperin, and D. R. Nelson, Phys. Rev. B **39**, 2344 (1989); A. V. Chubukov, S. Sachdev, and J. Ye, *ibid.* **49**, 11919 (1994).

[42] M. V. Sadovskii, Sov. Phys. JETP **39**, 845 (1974); Sov. Phys. Solid State **16**, 1632 (1974); Zh. Eksp. Teor. Fiz. **77**, 2070 (1979) [Sov. Phys. JETP **50**, 989 (1979)]; M. V. Sadovskii and A. A. Timofeev, J. Mosc. Phys. Soc. **1**, 391 (1991); for a detailed discussion of the formalism, see M. V. Sadovskii, *Diagrammatics* (World Scientific, Singapore, 2007).

[43] R. H. McKenzie and D. Scarratt, Phys. Rev. B **54**, R12709 (1996); O. Tchernyshyov, *ibid.* **56**, 3372 (1997).

[44] Y. Qi and S. Sachdev, Phys. Rev. B **81**, 115129 (2010).

[45] Y. Onose, Y. Taguchi, K. Ishizaka, and Y. Tokura, Phys. Rev. B **69**, 024504 (2004).

[46] A. J. Millis, A. Zimmers, R. P. S. M. Lobo, N. Bontemps, and C. C. Homes, Phys. Rev. B **72**, 224517 (2005).

[47] N. Armitage, P. Fournier, and R. Greene, arXiv:0906.2931, Rev. Mod. Phys. (to be published).

[48] Ar. Abanov, A. V. Chubukov, and A. Finkelstein, Europhys. Lett. **54**, 488 (2001); A. V. Chubukov and J. Schmalian, Phys. Rev. B **72**, 174520 (2005).

[49] Ar. Abanov, A. V. Chubukov, and M. R. Norman, Phys. Rev. B **78**, 220507(R) (2008).

[50] Y. Wang, L. Li, and N. P. Ong, Phys. Rev. B **73**, 024510 (2006).

[51] E. G. Moon and S. Sachdev, Phys. Rev. B **80**, 035117 (2009); see also R. K. Kaul, M. A. Metlitski, S. Sachdev, and C. Xu, *ibid.* **78**, 045110 (2008); V. Galitski and S. Sachdev, *ibid.* **79**, 134512 (2009).

[52] S. Sachdev, M. A. Metlitski, Y. Qi, and C. Xu, Phys. Rev. B **80**, 155129 (2009); S. Sachdev, arXiv:0910.0846 (unpublished).

[53] V. I. Belinicher, A. L. Chernyshev, A. V. Dotsenko, and O. P. Sushkov, Phys. Rev. B **51**, 6076 (1995).

[54] J. R. Schrieffer, J. Low Temp. Phys. **99**, 397 (1995); A. V. Chubukov, P. Monthoux, and D. K. Morr, Phys. Rev. B **56**, 7789 (1997).

[55] A. V. Chubukov and M. R. Norman, Phys. Rev. B **77**, 214529 (2008).

[56] J. R. Schrieffer, X. G. Wen, and S. C. Zhang, Phys. Rev. B **39**, 11663 (1989).

[57] A. V. Chubukov and D. M. Frenkel, Phys. Rev. B **46**, 11884 (1992).

[58] A. Singh and Z. Tesanovic, Phys. Rev. B **45**, 7258 (1992).

[59] A. V. Chubukov and K. A. Musaelian, Phys. Rev. B **51**, 12605 (1995).

[60] B. L. Altshuler, A. V. Chubukov, A. Dashevskii, A. M. Finkelstein, and D. K. Morr, Europhys. Lett. **41**, 401 (1998).

[61] I. S. Gradstein and I. M. Ryzhik, *Tables of Integrals, Series, and Products*, (Academic Press, San Diego, CA, 1994). Our $K(x)$

corresponds to $K(x^2)$ in Wolfram's "MATHEMATICA."

[62] H.-B. Yang, J. D. Rameau, P. D. Johnson, T. Valla, A. Tsvelik, and G. D. Gu, Nature (London) **456**, 77 (2008); J. Meng, G. Liu, W. Zhang, L. Zhao, H. Liu, X. Jia, D. Mu, S. Liu, X. Dong, W. Lu, G. Wang, Y. Zhou, Y. Zhu, X. Wang, Z. Xu, C. Chen, and X. J. Zhou, *ibid.* **462**, 335 (2009).

[63] C. C. Homes, S. V. Dordevic, G. D. Gu, Q. Li, T. Valla, and J. M. Tranquada, Phys. Rev. Lett. **96**, 257002 (2006); T. Valla, *ibid.* **96**, 119701 (2006).

[64] B. Kyung, J.-S. Landry, and A.-M. S. Tremblay, Phys. Rev. B **68**, 174502 (2003).

[65] P. Krotkov and A. V. Chubukov, Phys. Rev. Lett. **96**, 107002 (2006); Phys. Rev. B **74**, 014509 (2006).

[66] M. Khodas and A. Tsvelik, arXiv:1001.0590 (unpublished).